

PRODUCTION OF HEAVY QUARK BOUND STATES
IN HADRON-HADRON COLLISIONS

L. Camilleri
CERN
Geneva, Switzerland

Summary

The topics covered by this talk are listed below.

1. Production of the charmonium P-states (also known as χ -states) in hadronic collisions and as detected through their decay into a J/ψ and a photon.
2. Energy (\sqrt{s}) dependence of the production of the T family of resonances including a comparison with the J/ψ excitation curve and with some theoretical models.
3. Production of the T's in πp collisions.
4. Differences between the T and continuum dimuon events of similar mass.

1. Charmonium P-states (χ -states)

These states were first observed in e^+e^- storage rings ¹⁾ in the cascade reaction (Fig. 1)

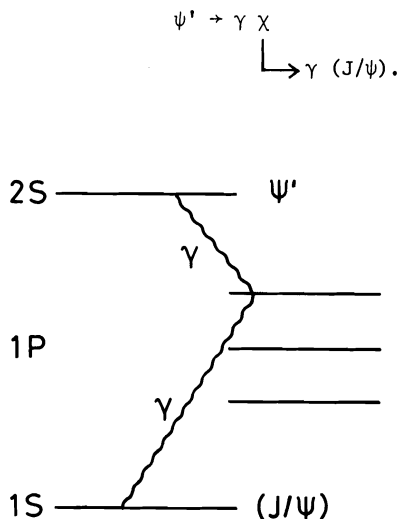


Fig. 1 - The cascade reaction $\psi' \rightarrow \gamma \chi \rightarrow \gamma (J/\psi)$.

Their masses, branching ratios into (J/ψ) and spin assignments are listed in Table I. The ratio $\sigma(\psi' \rightarrow \ell^+\ell^-)$ is of the order of 0.02 in hadronic collisions. After taking into account the branching ratios of the ψ' and J/ψ into $\ell^+\ell^-$ $\sigma(\psi')/\sigma(J/\psi)$ is still only 0.15 even at large \sqrt{s} where threshold effects due to the higher mass of the ψ' are no longer important. In order to explain the large number of J/ψ 's produced relative to ψ' 's it was

Table I. Properties of P-states

Mass (MeV/c)	Spin	B.R. to $(J/\psi) \gamma$ (%)
3413	0^+	3
3508	1^+	23
3554	2^+	16

postulated ²⁾ that

- a) (J/ψ) 's are produced from the gluons in the hadrons
- b) (J/ψ) 's are produced via the intermediate χ -states decaying into a J/ψ and a photon (Fig. 2).

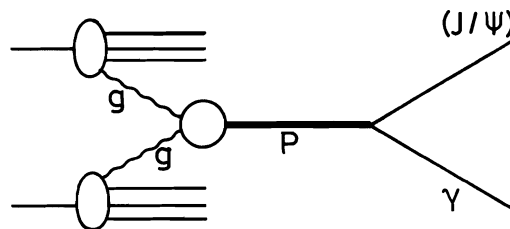


Fig. 2 - The production of (J/ψ) 's in hadronic collisions through an intermediate P-state.

If so, the magnitude of this effect can be measured by simply observing photons in association with J/ψ and reconstructing the $(J/\psi) \gamma$ effective mass.

Four experiments, two in $p-p$ collisions and two in $\pi-p$ collisions, have attempted to do this.

- i) Experiment R-806 (A^2 BCS) at the ISR measured ³⁾ J/ψ 's produced at $\sqrt{s} = 62$ and at $x_F \sim 0$ and decaying into e^+e^- . Their apparatus, Fig. 3, consisted of four identical modules. Each module consisted of a segmented liquid argon calorimeter and two Lithium transition radiation detectors. A module covered the angular range $50^\circ < \theta < 130^\circ$, $\Delta\phi = 40^\circ$ and had an acceptance of 1 sr. The π/e discrimination came from the pulse height in the transition radiation detector and from the pattern of energy deposition in the liquid argon calorimeter. Events with an invariant mass $2.67 < M_{ee} < 3.52 \text{ GeV}/c^2$ were taken to be (J/ψ) 's.

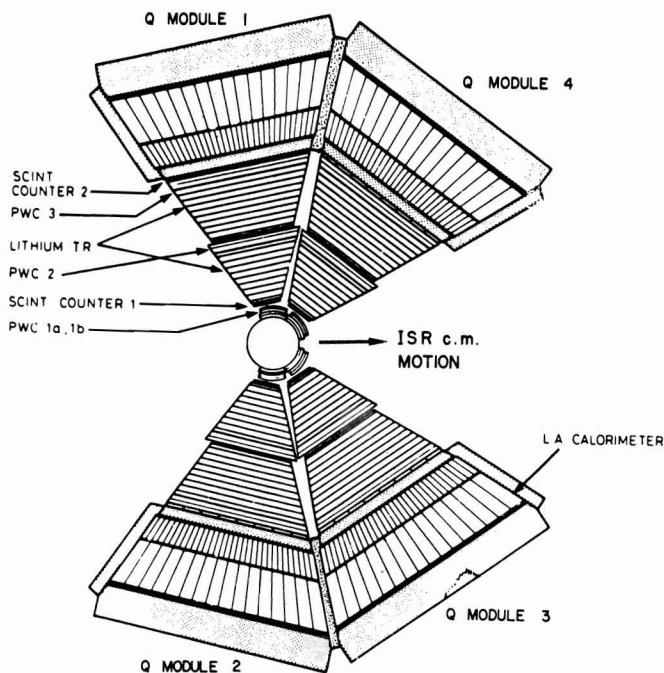


Fig. 3 - Apparatus of experiment R-806 at the ISR.

Since their resolution on the J/ψ comes almost entirely from the energy measurement of the two electrons, the direction of the two electrons and the mass of the J/ψ (3.097) were fixed and the energy of the two electrons were adjusted accordingly.

The invariant mass of the J/ψ 's with any photon of energy, E_γ , greater than 400 MeV was then formed. (Below 400 MeV the energy resolution and reconstruction efficiency for photons were poor). The invariant mass distribution is shown in Fig. 4a. The dashed line is a measure of the background obtained by mixing J/ψ 's with photons from events with

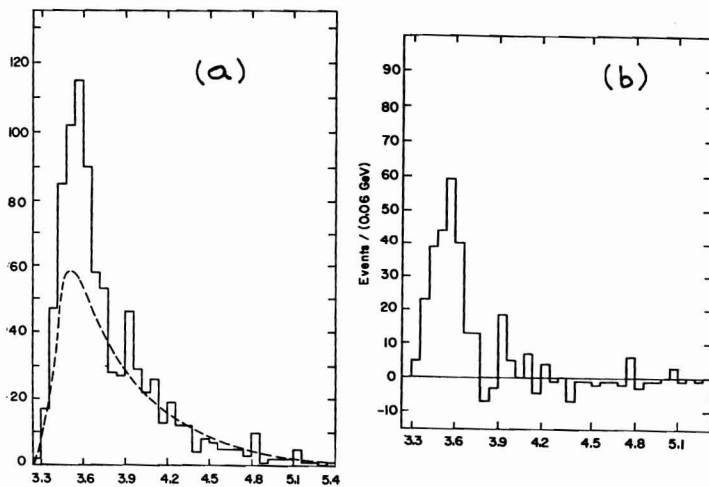


Fig. 4 - The $(J/\psi) \gamma$ invariant mass distribution for experiment R-806 before and after background subtraction.

a similar trigger (not necessarily J/ψ), and normalizing the resulting curve above $3.9 \text{ GeV}/c^2$. The difference between the two curves is shown in Fig. 4b. (Note that the method breaks down if the photon spectrum of the J/ψ events is different from the photon spectrum of background events). The excess of events around $3.5 \text{ GeV}/c^2$ is attributed by the authors to the χ states.

The fraction F_χ of J/ψ events originating from χ decays is found to be $(47 \pm 8)\%$. It is not possible to determine which of the 3510 and 3555 states contribute to the enhancement. The 3413 state is however ruled out, perhaps not surprisingly, in view of its small branching ratio to $(J/\psi) \gamma$ and of the $E_\gamma > 400 \text{ MeV}$ cut.

ii) Experiment R-702 (CSZ) at the ISR also observed ⁴⁾ the J/ψ at $\sqrt{s} = 62$, $x_F \sim 0$ and decaying into e^+e^- . Their apparatus, Fig. 5, consisted of a double arm spectrometer. Each arm subtended 0.5 sr and consisted of drift chambers before and after a magnet, an air filled Cerenkov counter (π -threshold at $5.8 \text{ GeV}/c$) and an array of 138 lead glass blocks.

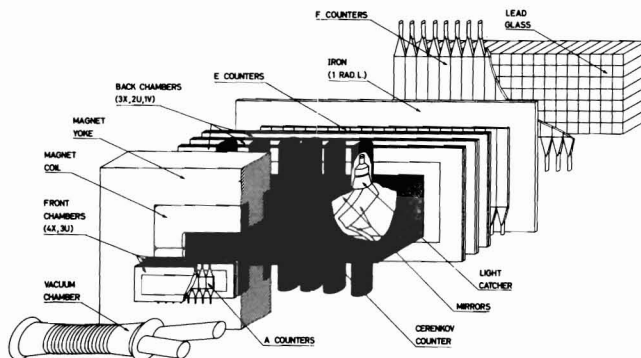


Fig. 5 - Apparatus of experiment R-702 at the ISR.

The rejection against pion pairs was $10^6 - 10^8$ and came from the Cerenkov counter and from the requirement of equality between the electron candidate momentum as measured in the magnet and its energy as measured in the lead glass.

Photons with energy greater than 150 MeV were then used to form the $(J/\psi) \gamma$ mass plot shown in Fig. 6. Events with two photons reconstructing to the π^0 mass were not used. The solid line is the background as estimated by mixing J/ψ 's with photons from different J/ψ events. No χ signal is observed and a value $F_\chi = 15^{+10}_{-15} \%$ is quoted.

iii) The FHIOT collaboration measured ⁵⁾ the J/ψ in π^-p collisions at $217 \text{ GeV}/c$ at Fermilab in the region $0 < x_F < 0.8$. Their mean x_F was 0.45 and the

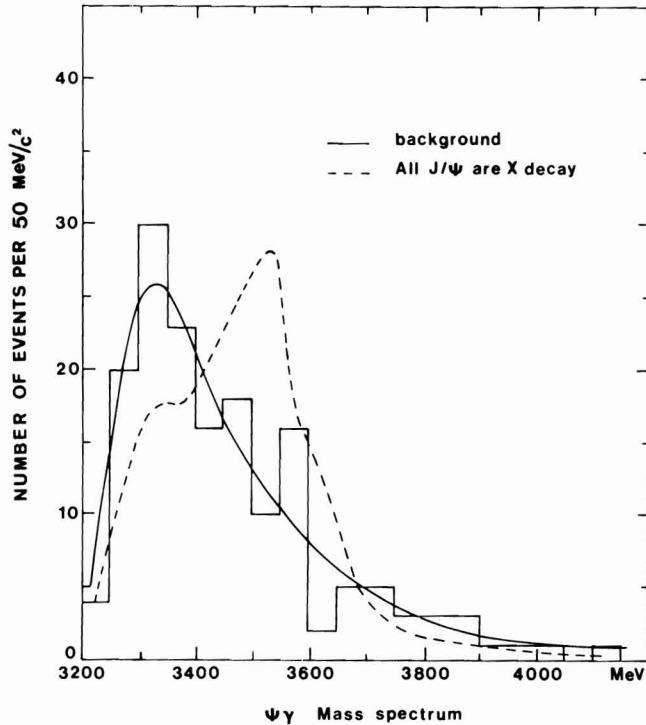


Fig. 6 - The $(J/\psi)\gamma$ invariant mass distribution for experiment R-702.

$\mu^+\mu^-$ decay mode was used.

The apparatus, (Fig. 7) consisted of a target made up of 2.5 cm Be followed by 40 cm liquid hydrogen, the Chicago cyclotron magnet, 76 lead-glass blocks to detect the photons and a steel hadron absorber.

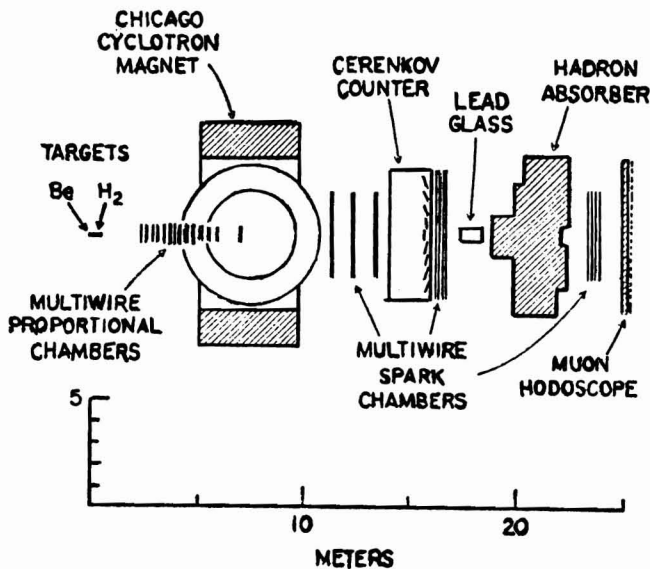


Fig. 7 - Apparatus of the FHIOT collaboration at Fermilab.

Photons with $E_\gamma > 5$ GeV were used (γ 's from χ 's have $E_\gamma > 10$ GeV) and π^0 's were rejected. The background was estimated in two ways

- By mixing (J/ψ) 's with γ 's associated with events with dimuon mass outside the (J/ψ) region.
- By measuring the spectrum of π^+ and π^- associated with (J/ψ) 's taking the average of these two spectra as representing π^0 's and doing a Monte Carlo calculation to determine the number of γ 's from π^0 's in association with (J/ψ) 's.

The two methods gave consistent results. The $(J/\psi)\gamma$ invariant mass spectrum is shown in Fig. 8 together with the background. An excess of events is observed yielding a value for F_χ of $(70 \pm 28)\%$. Fitting a gaussian to the excess of events yields a mass of (3.51 ± 0.02) GeV/c^2 .

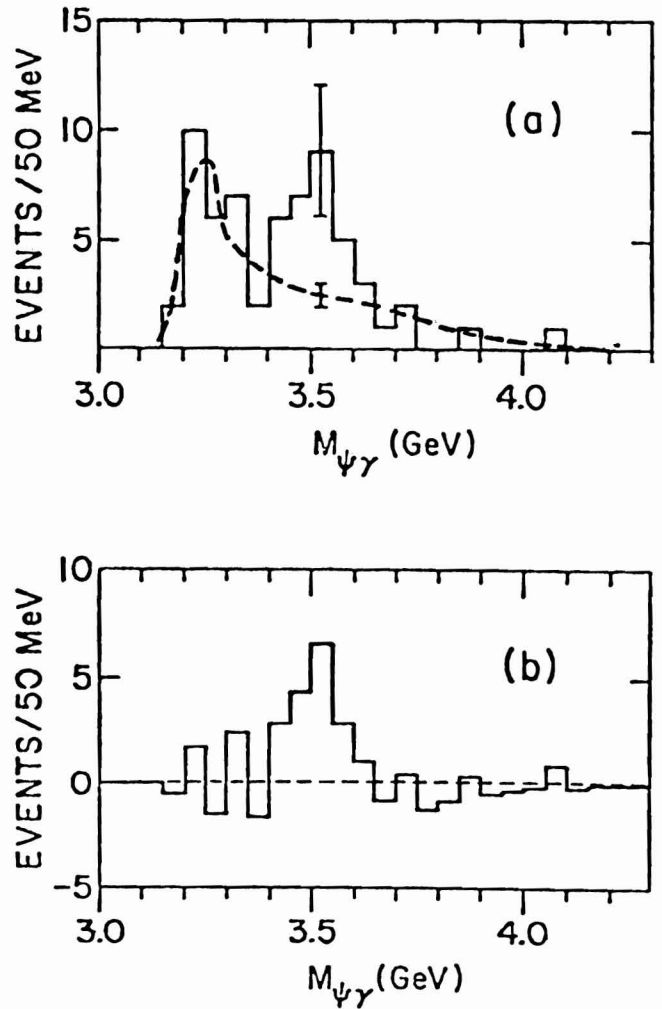


Fig. 8 - The $(J/\psi)\gamma$ invariant mass distribution obtained by the FHIOT collaboration.

iv) Experiment WA-11 (SISI) at the SPS measured ⁶⁾ (J/ψ)'s produced in π^-p collisions at 150 and 175 GeV/c incident beam momentum and in the range $-0 < x_F < 0.6$ using the $\mu^+\mu^-$ decay mode.

Their apparatus, (Fig. 9), the GOLIATH magnetic spectrometer, consisted of three Be targets, MWPC's, shower counters and an iron hadron absorber. They observe a narrow J/ψ and ψ' .

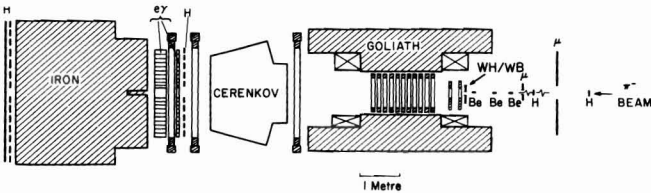


Fig. 9 - The GOLIATH Magnetic Spectrometer.

In contrast to the other three experiments only γ 's converted in the target, scintillators and MWPC's (a total of 22% R.L.) are used. In this way the magnetic spectrometer can be used to measure the two conversion electrons with very good accuracy. The background is once again estimated by mixing the γ 's with the four preceding J/ψ 's. Their results are shown in Fig. 10. A peak is observed at 3520 MeV/c². This is incompatible with the $\chi(3413)$ and $\chi(3554)$. Their value of F_χ is $(11.0 \pm 3.6)\%$.

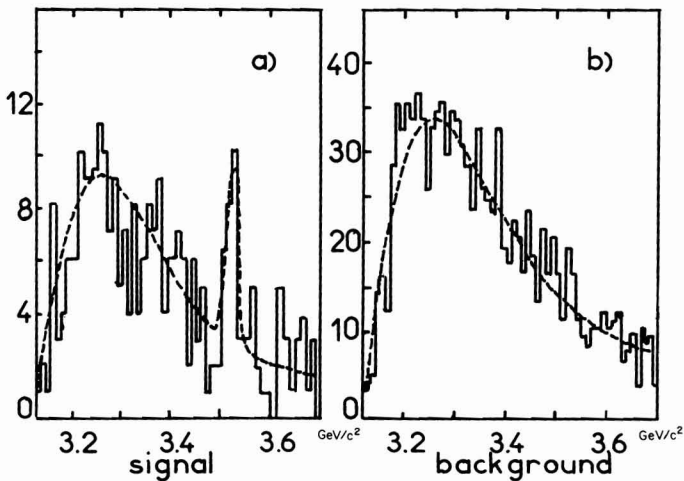


Fig. 10 - The (J/ψ) γ invariant mass distribution obtained by the SISI collaboration.

The results from the four experiments are summarised in Table II and are somewhat inconsistent. However this is not surprising given the differences in initial states, \sqrt{s} and x_F . More experiments are needed especially some with enough resolution to distinguish between the three χ states.

Table II. Summary of results on the production of J/ψ 's via P-states.

Experiment	Initial state	\sqrt{s} (Momentum)	$\langle x \rangle$	J/ψ decay mode used	F_χ (%)
Ref. 3	pp	62	0	e^+e^-	47 ± 8
Ref. 4	pp	62	0	e^+e^-	15^{+10}_{-15}
Ref. 5	π^-p	20 (217)	0.45	$\mu^+\mu^-$	70 ± 28
Ref. 6	π^-p	18 (150,175)	0.2	$\mu^+\mu^-$	11.0 ± 3.6

2. \sqrt{s} Dependence of the T in p-p collisions.

Five experiments, one at FNAL, one at the SPS and three at the ISR have contributed results to this reaction.

i) The CFS collaboration (Fig. 11) following their discovery of the T have measured its cross-section ⁷⁾ at incident beam momentum 200, 300, 400 GeV/c ($\sqrt{s} = 19.4, 23.7$ and 21.4 respectively). They observe the T through its $\mu^+\mu^-$ decay mode. Their mass resolution was $\pm 2.2\%$ at first and was later improved to $\pm 1.7\%$ in some special running to confirm the T'' . From their own fit they quote $M_{T'} - M_T = 0.57 \pm 0.03 \text{ GeV}/c^2$

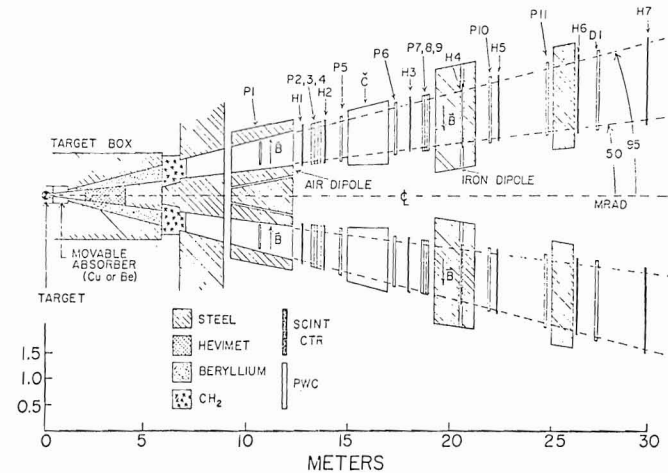


Fig. 11 - Apparatus of the CFS collaboration.

and using the splitting observed at DORIS, $M_{T'} - M_T = 0.555 \pm 0.011 \text{ GeV}/c^2$, they observe the T'' as an 11 st. dev. effect (Fig. 12).

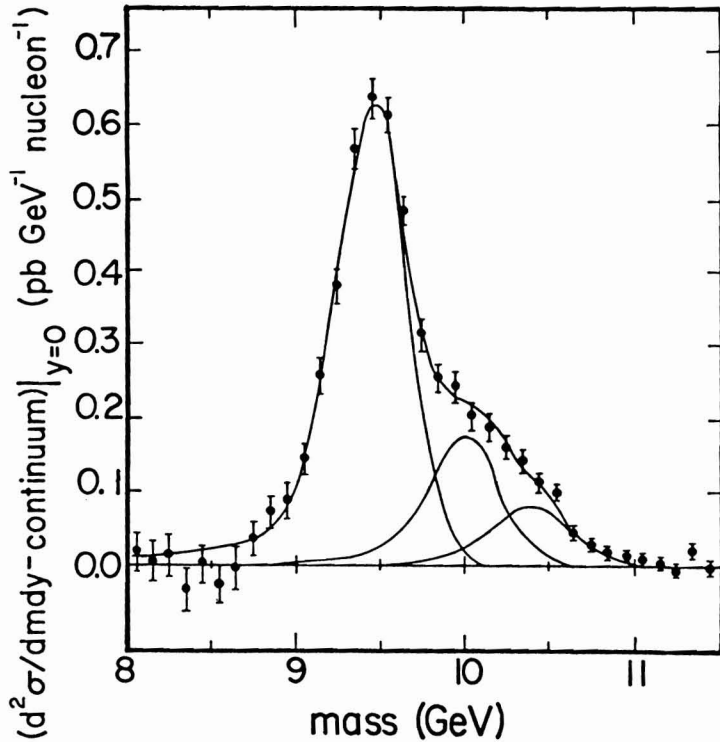


Fig. 12 - The CFS mass spectrum, continuum subtracted and showing a 3-resonance fit.

The cross-sections they measure are listed in Table III for the sum of the 3 peaks.

Table III

T Cross-sections obtained by the CFS collaboration

Momentum (GeV/c)	y	$B \frac{d\sigma}{dy} _{y=0}$ (T + T' + T'') (cm ²)
400	0.0	$(0.44 \pm 0.06) \times 10^{-36}$
300	0.2	$(0.14 \pm 0.03) \times 10^{-36}$
200	0.4	$(0.003 \pm 0.003) \times 10^{-36}$

ii) Experiment R-108 (CCOR collaboration) at the ISR measured the T at $\sqrt{s} = 62$ and 44 GeV, through its e^+e^- decay mode⁸). The apparatus, Fig. 13, consists of a superconducting solenoid containing cylindrical drift chambers and two arrays of lead glass outside the magnet. The e^+e^- mass is obtained from the energy of the two electrons as measured in the lead glass and a $\Delta M/M \sim \pm 4\%$ at 10 GeV/c² has been achieved. The π/e discrimination comes from requiring a track of momentum p to point to a cluster of energy E such that $E \sim p$ within the measurement errors and also from the pattern of energy deposition in the lead glass. The background estimated from the number of e-pair candidates of same charge

amounts to 10% at the T. Their cross-sections are shown in Fig. 14 and after subtraction the continuum the T cross sections are found to be : -

$$\begin{aligned} \sqrt{s} = 62 \quad B \frac{d\sigma}{dy} |_{y=0} &= (9 \pm 3) \times 10^{-36} \text{ cm}^2 \\ &\text{on 40 events} \\ \sqrt{s} = 44 \quad B \frac{d\sigma}{dy} |_{y=0} &= (6 \pm 3) \times 10^{-36} \text{ cm}^2 \\ &\text{on 6 events.} \end{aligned}$$

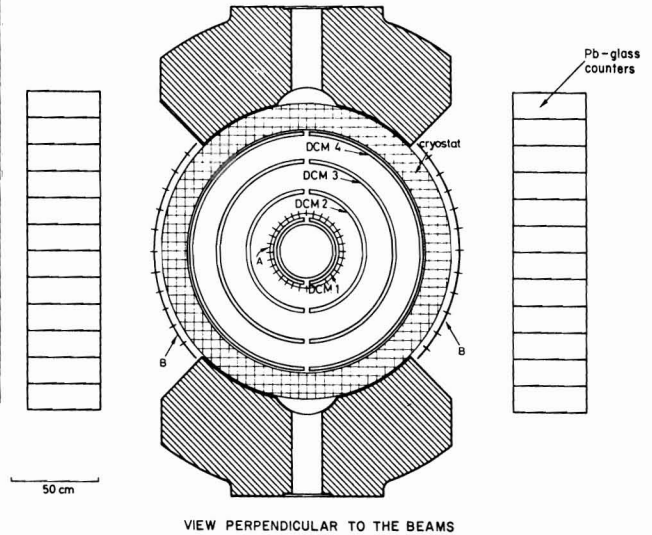


Fig. 13 - Apparatus of the CCOR collaboration.

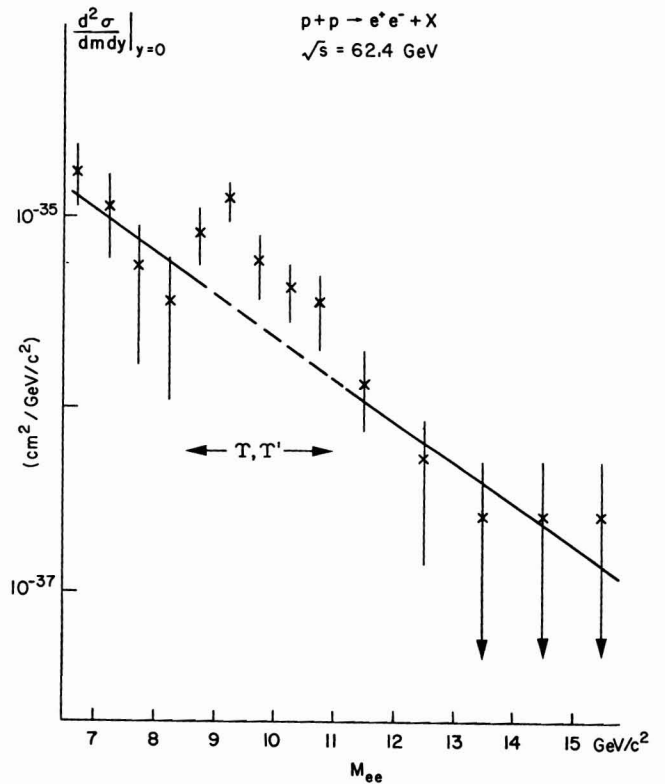


Fig. 14 - Cross-sections obtained by the CCOR Collaboration.

iii) Experiment R-209 at the ISR measured ⁹⁾ the T into $\mu^+\mu^-$ at $\sqrt{s} = 62$ using an apparatus, Fig. 15, consisting of magnetised iron toroids, drift chambers and an inner detector to study associated particles and give the initial directions of the muons. The iron toroids are used both for momentum measurement and for

hadronic filters. The experiment covers a large x_F range ($-0.3 < x_F < 0.6$) and has an acceptance of 10.5% of σ_{tot} . Their mass resolution is $\Delta M/M = \pm 10\%$. No background survives at the T and they quote

$$B \frac{d\sigma}{dy} \Big|_{y=0} = (10 \pm 4) \times 10^{-36} \text{ cm}^2$$

and

$$B\sigma_{tot} = (15 \pm 6) \times 10^{-36} \text{ cm}^2 \text{ on about 100 events (Fig. 16).}$$

iv) Experiment R-806 also at the ISR measured ¹⁰⁾ the T into e^+e^- and $\sqrt{s} = 62$ and 53. The apparatus was described in section 1(i). Their mass resolution was $\pm 3.8\%$ and the background was estimated to be 12% at the T . Their mass spectrum is shown in Fig. 17 and their cross-sections are

$$\sqrt{s} = 62 \quad B \frac{d\sigma}{dy} \Big|_{y=0} = (15.2 \pm 5.5) \times 10^{-36} \text{ cm}^2 \text{ on 45 events}$$

$$\sqrt{s} = 52 \quad B \frac{d\sigma}{dy} \Big|_{y=0} = (13.5 \pm 7.4) \times 10^{-36} \text{ cm}^2 \text{ on 7 events.}$$

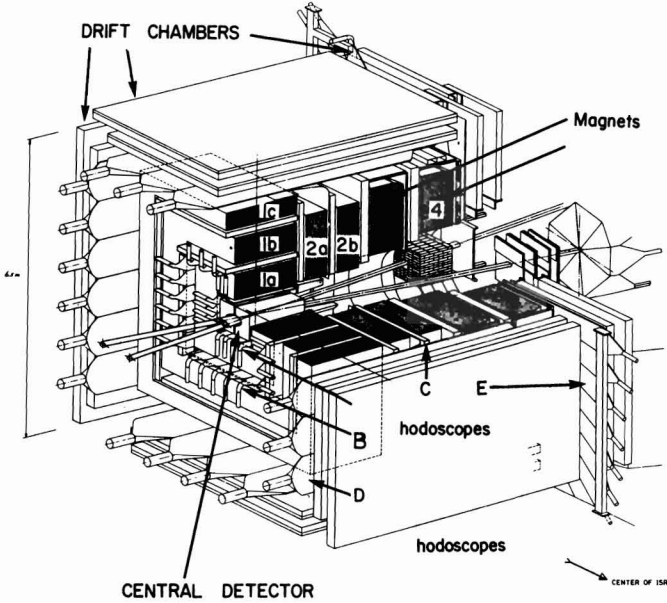


Fig. 15 - Apparatus of experiment R-209 at the ISR.

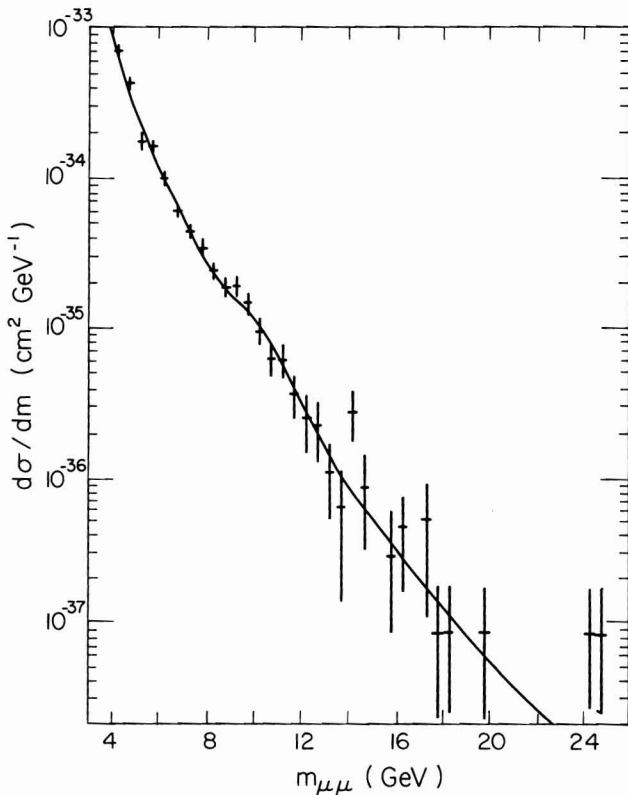


Fig. 16 - Cross-sections obtained in experiment R-209.

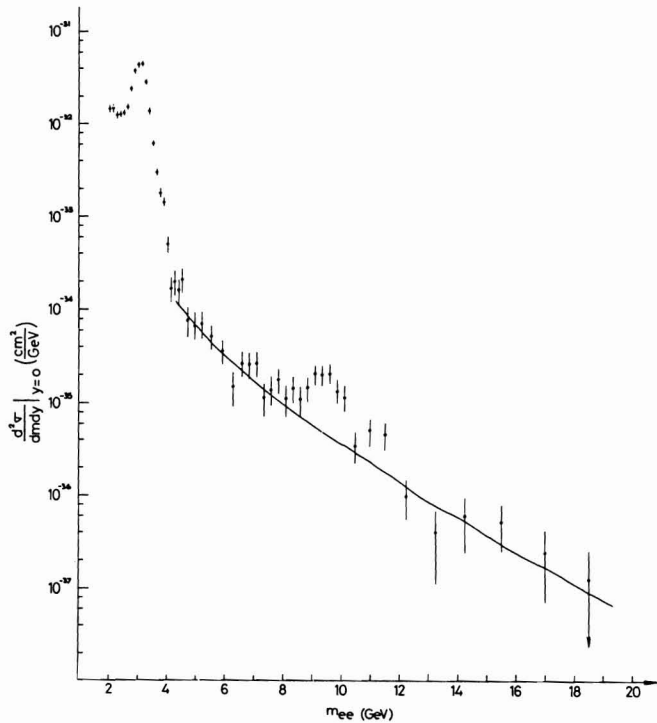


Fig. 17 - Mass spectrum obtained in experiment R-806.

v) Experiment NA-3 at the CERN SPS, an experiment which has so far concentrated on pion production of dimuons ¹¹⁾ (see section 3) also observed a few T 's at 200 GeV/c incident proton momentum ($\sqrt{s} = 19.4$) and they quote

$$B \frac{d\sigma}{dy} \Big|_{y=0} = (3.8 \pm 3.2) \times 10^{-38} \text{ cm}^2.$$

These results are combined into an excitation curve on Fig. 18. The solid line is the J/ψ excitation curve divided by a factor of 500. The agreement in shape is remarkable. The factor of 500 can be compared with a prediction of Gaisser et al. ¹²⁾ for the

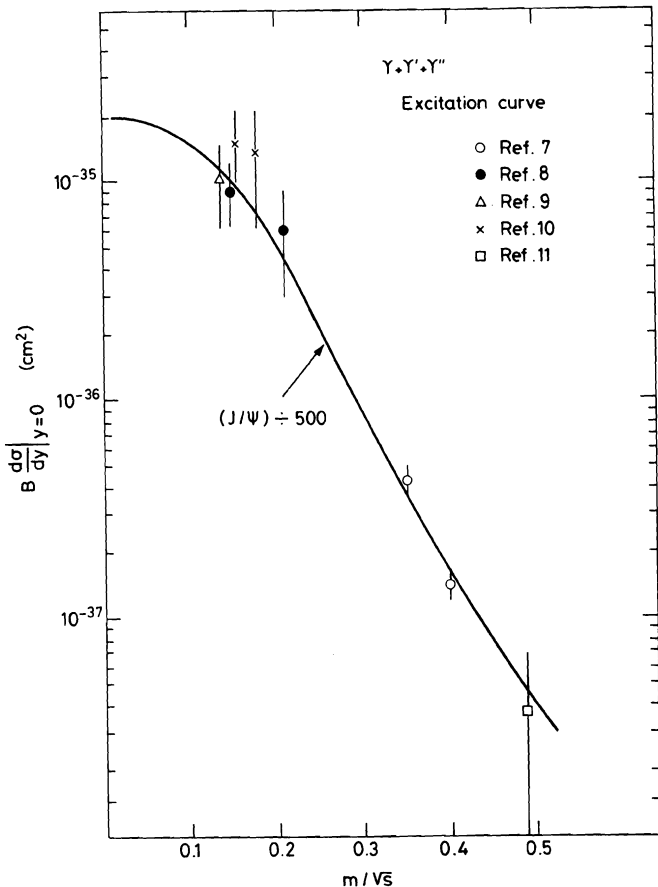


Fig. 18 - T excitation curve and comparison with the J/ψ curve.

production cross-section of heavy $q \bar{q}$ bound states, Q :-

$$B(Q \rightarrow \ell^+ \ell^-) \sigma = \frac{1}{M_Q^3} \Gamma_Q \rightarrow \ell^+ \ell^- F(M_Q/\sqrt{s})$$

where M_Q and Γ_Q are respectively the mass and leptonic width of the state Q , and F is a universal function of M_Q/\sqrt{s} , the same function for all heavy $q \bar{q}$ states.

Using the T and J/ψ leptonic widths measured by the e^+e^- storage rings, namely $\Gamma_T \rightarrow e^+e^- = 1.33$ KeV and $\Gamma_{J/\psi} \rightarrow e^+e^- = 4.69$ KeV, one obtains

$$B \sigma_{J/\psi} / B \sigma_T = 100$$

which is a factor of 5 lower than observation.

Lastly, in Fig. 19, the excitation curve is compared to two calculations by Owens and Reya ¹³⁾ one based on light quark fusion and another in which both light quark fusion and gluon fusion are included. In

both cases the curves are normalised to the CFS $\sqrt{s} = 27.4$ GeV point. The curve for light quark fusion only tends to be below most of the ISR points.

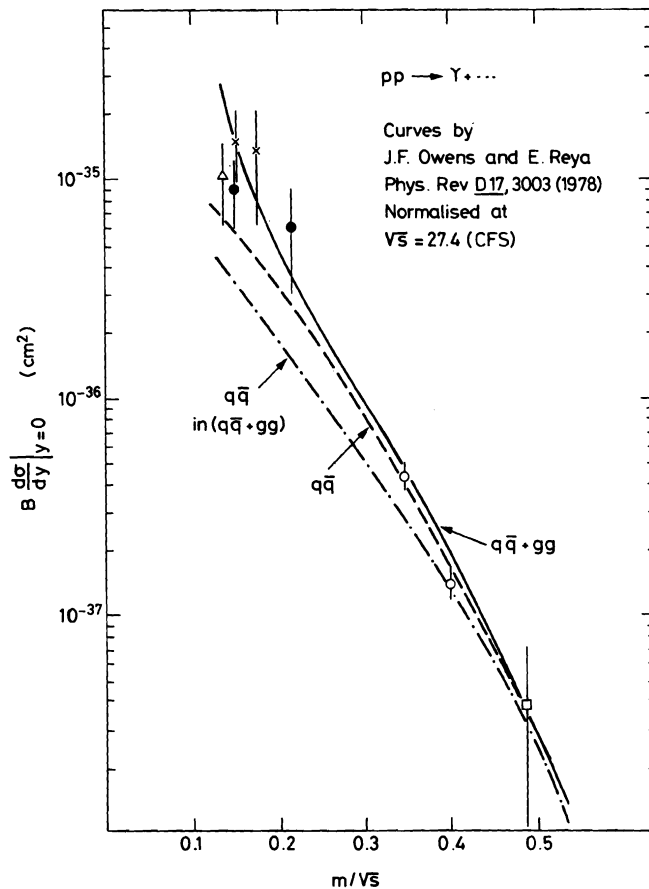


Fig. 19 - Comparison of T excitation curve to a model including light quark fusion and gluon fusion.

On the other hand if gluon fusion is added a slightly better fit is obtained. Also shown on Fig. 19 is the $q \bar{q}$ contribution to the cross-sections when both $q \bar{q}$ and $g g$ fusion are included. It may be of interest to note that according to this calculation at the ISR only 18% of the cross-section comes from $q \bar{q}$ fusion whereas at $\sqrt{s} = 27.4$ this amounts to 55%.

3. Production of T 's in π - p collisions.

The only experiment to have observed T 's in π - p collisions is experiment ¹¹⁾ NA-3 at the SPS.

They see the T in its $\mu^+\mu^-$ decay mode in π^- - p collisions at 200 and 280 GeV/c and π^+ - p at 200 GeV/c. The beam is unseparated but the incident particles are identified with a system of differential and threshold Cerenkov counters. The apparatus, Fig. 20, consisted of a platinum target upstream of a tungsten-uranium-steel beam dump, followed by superconducting dipole MWPC's and finally a hadron

NA 3 SPECTROMETER

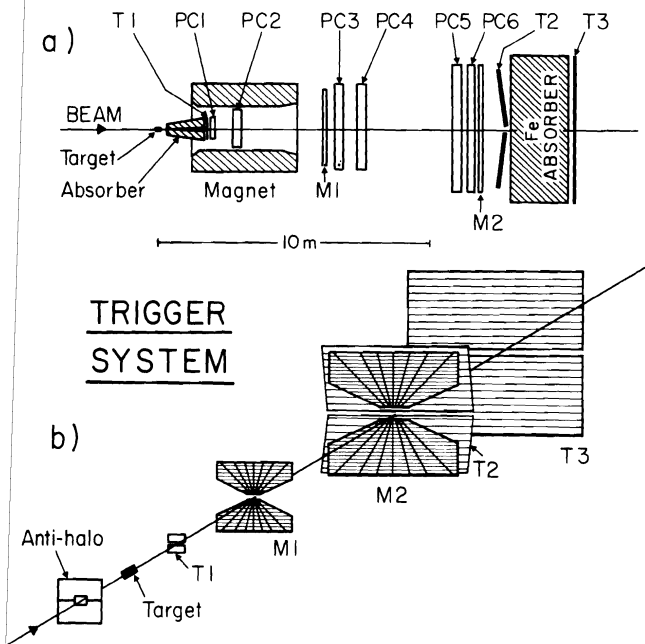


Fig. 20 - Apparatus of experiment NA-3 at the SPS.

absorber (12 cm Pb plus 1.8 m Fe). The mass resolution at the upsilon is $\pm 4.5\%$. The mass spectrum for the π^+p data (Fig. 21) shows a clear T peak whereas in the π^-p spectra (Figs. 22a, b) the T is less predominant due to the higher Drell-Yan continuum. Fits to the data with four parameters: -

- α the ratio of ($T + T' + T''$) to the continuum at $9.46 \text{ GeV}/c^2$.
- The relative abundance of the T' and T'' with respect to the T .
- The slope parameter b in e^{-bM} for the continuum,

yield the number of events, cross-sections and ratios to the continuum shown in Table IV. The previous upper limit ¹⁴⁾ in π^-p collisions at $225 \text{ GeV}/c$ was $B \sigma < 1.4 \text{ p barn/nucleon}$ using an A -dependence of 1.12.

The following conclusions can be drawn:

- The ratio $\sigma(\pi^-p \rightarrow T + \dots) / \sigma(\pi^+p \rightarrow T + \dots) = 0.76 \pm 0.29$ at 200 GeV .
- The ratio of T to the continuum is 4.2 ± 1.0 in π^+p and 0.87 ± 0.26 in π^-p showing that the continuum level is much higher in π^-p whereas the T cross-section is about the same in π^-p and π^+p . When looking for enhancements one is therefore better off using π^+ collisions.
- $\sigma(p p \rightarrow T \dots) / \sigma(\pi^+p \rightarrow T + \dots) = 0.03 \pm 0.02$ at $200 \text{ GeV}/c$ indicating that

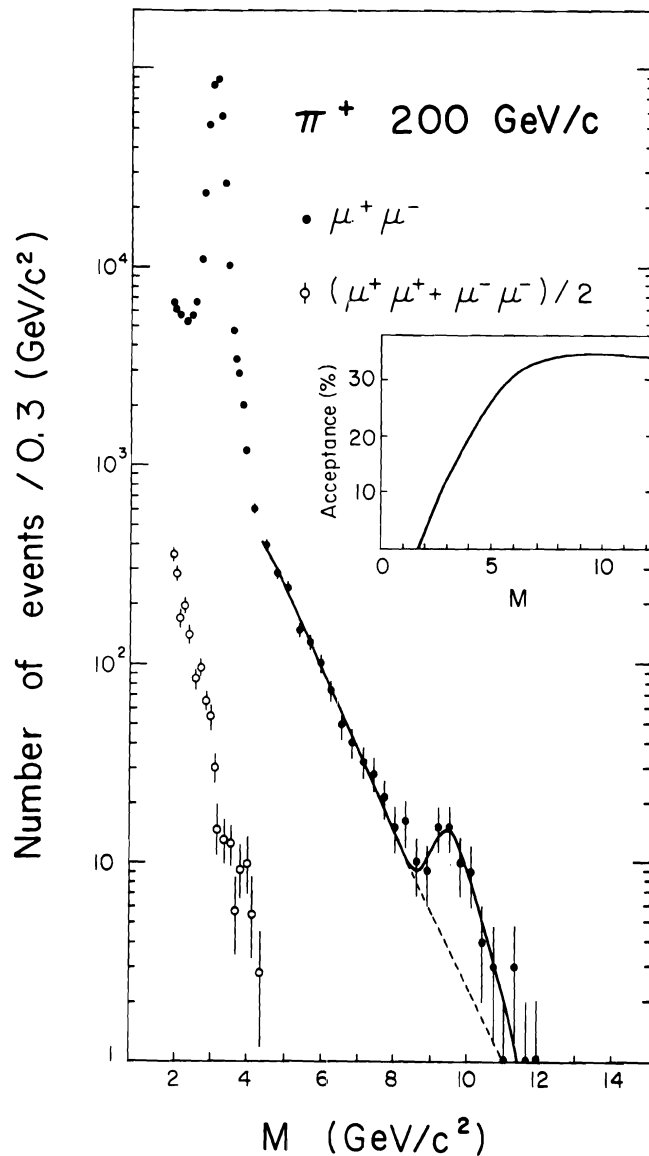


Fig. 21 - Dimuon mass spectrum obtained in π^+p collisions by experiment NA-3.

π^+ 's are much more efficient than protons at producing T 's.

- The calculation of Owens and Reya ¹³⁾ using $g g$ and $q \bar{q}$ fusion comes within a factor of 1.5 of predicting the π^-p cross-sections when fixing the normalisation at the CFS $400 \text{ GeV}/c$ $p p$ point.

4. Differences between the T and the continuum.

- Ratio of T to the continuum.

In $p p$ collisions

$$R_{pp} = B \left. \frac{d\sigma}{dy} \right|_{y=0} (T + T' + T'') / \left. \frac{d^2\sigma}{dm dy} \right|_{y=0} (m = m_T)$$

goes from 0.1 at $\sqrt{s} = 20$ to ~ 3 at $\sqrt{s} = 62$.

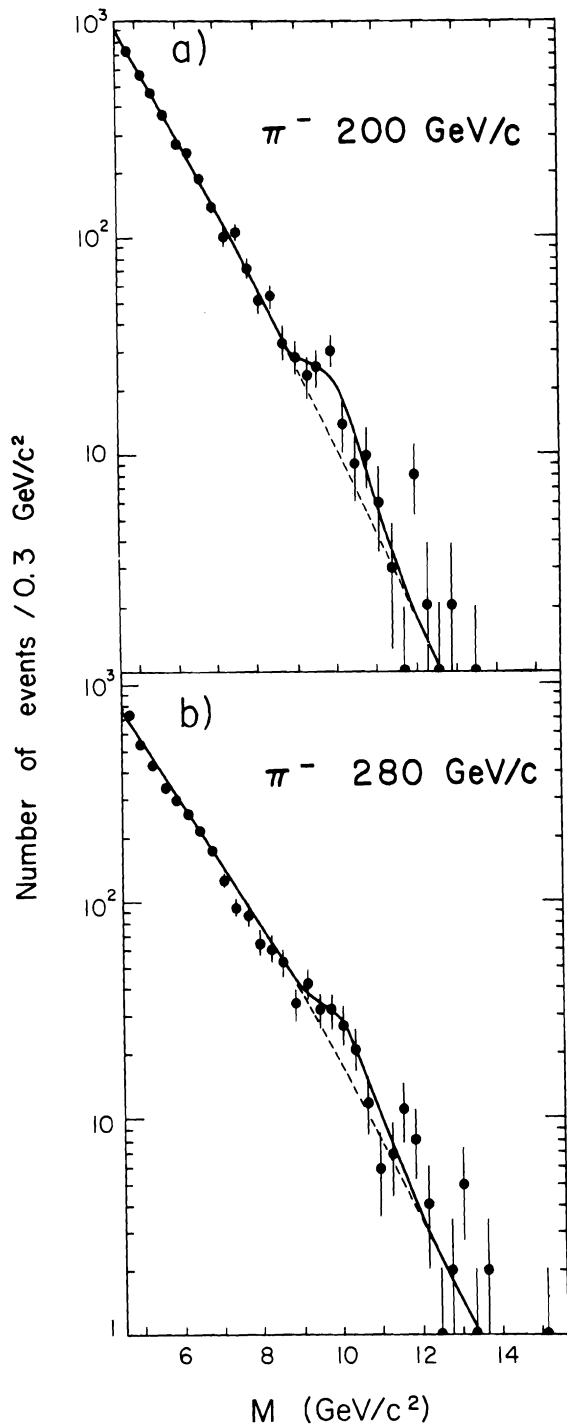


Fig. 22 - Dimuon mass spectrum obtained in $\pi^- p$ collisions by experiment NA-3.

($\div 1.45$ for the T alone).

In contrast at DORIS

$$R_{ee} = \int B \sigma_{ee}(T) dE / \sigma(e^+e^- \rightarrow \mu^+\mu^-)_{E=m_T}$$

$$< 0.022 \text{ using } B(T \rightarrow \mu^+\mu^-) \sim (2.2 \pm 2.0)\%.$$

The production of T's in p-p collisions is therefore not electromagnetic in origin.

ii) Decay distributions.

Fitting decay distributions to $1 + \lambda \cos^2\theta^*$ yields the values of λ listed in table IV for both the continuum and the T. Although the errors on the individual experiments are large, it is of interest to note that on the whole the values of λ obtained for the T are smaller than those for the continuum. In the continuum $\lambda=1$ is likely whereas for the T $\lambda=0$ is favoured.

Table IV

\sqrt{s}	19.4	19.4	22.9
Particle	π^+	π^-	π^-
	200 GeV/c	200 GeV/c	280 GeV/c
Events (T, T', T'')	53 \pm 12	55 \pm 15	66 \pm 20
$B \frac{d\sigma}{dy} _{y=0.2}$ (T, T', T'')	2.7 \pm 0.9	2.1 \pm 0.7	3.4 \pm 1.3
pb/nucleon			
$B \sigma$ (T, T', T'')	1.9 \pm 0.6	1.5 \pm 0.5	2.4 \pm 0.9
pb/nucleon			
T's/cont..(9.46)	4.2 \pm 1.0	0.87 \pm 0.26	0.70 \pm 0.22

Table V. Decay parameter for the T and the continuum.

Experiment	λ_T	$\lambda_{cont.}$
R-209	0.6 \pm 1.0	1.0 \pm 0.3
R-806	0.79 \pm 0.43	1.15 \pm 0.34
R-806 (continuum subtracted)	0.31 \pm 0.28	
NA-3 (π^+)	0.12 \pm 0.77	

iii) p_T spectrum.

The values of the mean p_T , $\langle p_T \rangle$, for the T and for neighbouring continuum regions are listed in Table VI. Here again differences are observed: the mean p_T , $\langle p_T \rangle$ of the T tends to be higher than for the continuum at all \sqrt{s} . This is clearly illustrated by the CFS data at 400 GeV/c shown in Fig. 23. The differences seem to arise mostly at large p_T .

Table VI. $\langle p_T \rangle$ for the T and the continuum.

Experiment	$\langle p_T \rangle_T$	$\langle p_T \rangle_{cont.}$
CFS (400)	1.48 \pm 0.04	1.20 \pm 0.02
(300)	1.13 \pm 0.05	1.03 \pm 0.05
R-108	1.8 \pm 0.2	1.6 \pm 0.3
R-209	1.8 \pm 0.2	
R-806	1.95 \pm 0.28	1.43 \pm 0.09

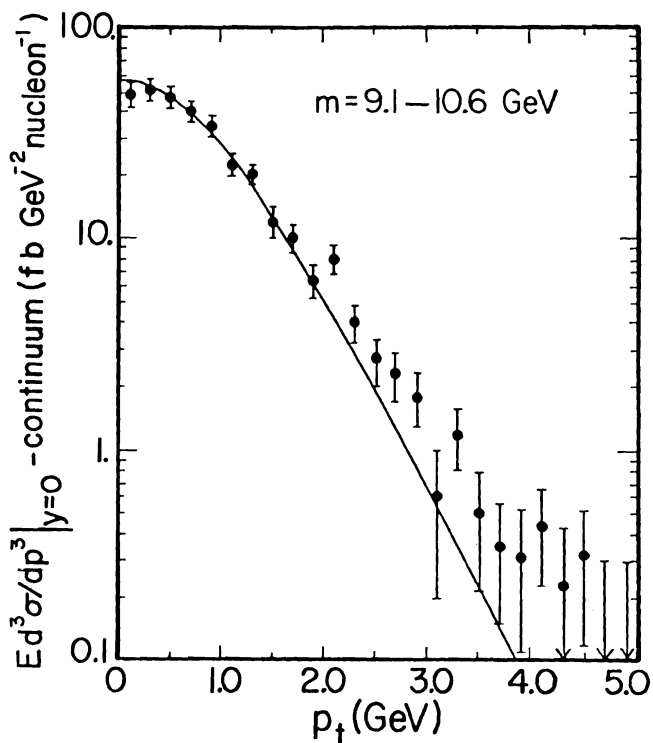


Fig. 23 - Dimuon p_T spectrum obtained by CFS in the upsilon region compared to a continuum p_T spectrum.

REFERENCES

- 1) W. Braunschweig et al., Phys. Lett. 57B, 407 (1975).
G. Feldman et al., Phys. Rev. Lett. 35, 821 (1975).
- 2) C.E. Carlson and R. Suaya, Phys. Rev. D14, 3115 (1976).
S.D. Ellis et al., Phys. Rev. Lett. 36, 1263 (1976).
- 3) C. Kourkouvelis et al., Phys. Lett, 81B, 405 (1979).
- 4) A.G. Clark et al., Nucl. Phys. B142, 29 (1978).
- 5) T.B.W. Kirk et al., Phys. Rev. Lett. 42, 619 (1979).
- 6) Y. Lemoigne et al., Paper D-2, submitted to this symposium.
- 7) J.K. Yoh et al., Phys. Rev. Lett. 41, 684 (1978).
K. Ueno et al., Phys. Rev. Lett. 42, 486 (1979).
- 8) A.L.S. Angelis et al., Paper C-14, submitted to this symposium.
- 9) D. Antreasyan et al., Results submitted to this symposium.
- 10) C. Kourkouvelis et al., Results submitted to this symposium.
- 11) First Evidence for Upsilon production by Pions. J. Badier et al., submitted to Physics Letters.
- 12) T.K. Gaisser et al., Phys. Rev. D15, 2572 (1977).
- 13) J.F. Owens and E. Reya, Phys. Rev. D17, 3003 (1978).
- 14) K.J. Anderson et al., Phys. Rev. Lett. 42, 944 (1979).

DISCUSSION

- Q. (Irwin Gaines, Fermilab) If these new measurements are right and most of the J/ψ are not coming from χ decays, how does one now explain the suppression of ψ' production ?
- A. Well, first of all, I'm not sure that any of these measurements have decidedly ruled out the J/ψ 's coming from these χ states. I think the experiments are just simply inconclusive at the moment. You could certainly have up to 50% of the J/ψ 's coming from χ states.
- Q. (R. Raja, Fermilab) I have a comment to make on your χ production. The whole motive for the presentation was 2 gluon fusion model and using the two gluon fusion model you cannot produce the 1^{++} because it doesn't go into 2 gluons. You went to four different experiments and you finally concluded that it is consistent with 1^{++} . Since the data is so inconclusive at the moment the Fermilab-Harvard experiment would prefer if you interpreted it as to be consistent with 2^{++} .
- A. First of all I did mention that the authors themselves would prefer to stress the 2^{++} . The other thing is that I have spoken to several people and it is not clear that you cannot produce the 1^{++} with 2 gluons. Apparently there are some ways of doing it.
- Q. (Selove, Pennsylvania) Excuse me, the answer is probably trivial but in the production of T 's by π^+ or π^- I think I understand why the continuum production from π^+ is so much smaller than from π^- . Why is the T production from π^+ not smaller than π^- ? It is in fact bigger from your numbers.
- A. Yes, I think clearly they come from different production mechanisms.
- Q. But it's not single photon production presumably?
- A. No, that's what I ended up concluding. The T is not produced via a one-photon mechanism.
- Q. What other mechanisms are there that have been...
- A. Well, you can have the fusion not going through a photon but directly through some sort of hadronic state.
- Q. (J. Kirkby, SLAC) This question concerns whether χ states are present or not in the experimental data. This clearly depends crucially on to the validity of the background subtraction procedure. I would gain much more confidence if the experimenters would repeat their analysis but using events just below the ψ . These should not form a fixed invariant mass with any γ . Thus comparing the $\mu^+\mu^-\gamma$ spectrum where the γ is produced in the same event as the $\mu^+\mu^-$ with the $\mu^+\mu^-$ spectrum where the γ is produced in a different event should give a check as to how reliable this event-mixing method is. Has this check been made and if so what are the results ?
- A. I do not believe this particular check was made. However comparing the two spectra in the J/ψ events, and for those experiments that mix J/ψ and γ 's obtained in association with J/ψ the agreement is very good outside the χ region.
- Q. (John Ellis, CERN) I would like to try and at least give a personal answer to the question which was raised by Mr. Gaines about the relative rates of production of J/ψ and ψ' 's. In fact Mary K. Gaillard, Nanopoulos, Rudaz and myself wrote a paper in '77 at the same time as Gaisser et al. where we have the same scaling law for the production of these different resonances. And there we were able to explain to within a factor of 2 the relative production rate of ψ' and J/ψ without using the intermediate states at all. And the same models gave the correct results for ratio of T, T', T'' production.
- Q. (Lipkin, Weizmann Inst.) Is there any attempt to look at π^0 's together with the J/ψ to look for states which would decay by isospin violation into π^0/ψ .
- A. I'm not aware of any experiment that has tried to do that.